ISBN: 978-3-95450-208-0 doi:10.18429/JACoW-IPAC2019-TUPRB088

# GENERATION OF HIGH PEAK POWER HARD X-RAYS AT LCLS-II WITH DOUBLE BUNCH SELF-SEEDING

A. Halavanau, F.-J. Decker, C. Emma, G. Marcus, A.A. Lutman, Z. Huang, Y. Ding, D. Zhu, J. Krzywinski, C. Pellegrini[1]

[1] SLAC National Accelerator Laboratory, Stanford University, Menlo Park CA 94025, USA

*Abstract*

We propose to use existing LCLS copper S-band linac double bunch infrastructure to significantly improve LCLS-II hard X-ray performance. In our setup, we use the first bunch to generate a strong seeding X-ray signal, and the second bunch, initially traveling off-axis, to interact with the seed in the amplifier undulator and generate a near TW, 15 fs duration X-ray pulse in the 4 to 8 keV photon energy range. We investigate, via numerical simulations, the required transverse beam dynamics and the four crystals X-ray monochromator to be added to the existing LCLS-II beamline and discuss the final properties of the hard X-ray pulses and their potential application in high intensity, high-field physics experiments, including QED above the Schwinger critical field.

## INTRODUCTION

Recent developments in laser technology will open the avenue for previously unseen highly nonlinear regimes of light-light, and particle-light interactions [1,2]. At SLAC, such experiments are planned at FACET-II facility using the ultra-relativistic electron beam and a high power $CO_2$ laser. Recent numerical studies revealed that in double-bunch configuration one can significantly improve the X-ray FEL power to TW scale by tapering the amplifier section [3–9]. Furthermore, colliding TW X-ray pulse with GeV scale electron beam, one can increase the electric field strength in the electron rest frame by many orders of magnitude. To provide even larger electric field, one may further reduce the X-ray spotsize. For example, a 4 keV 1 TW X-ray pulse, focused down to 10 nm spotsize, yields $10^{15}$ V/m, a value similar to obtainable in a PW laser. When back-reflected and collided with GeV-scale electron beam, the field gradient in the electron rest frame is increased by a factor of $\gamma$ or $10^4$ times, providing maximum of $10^{19}$ V/m, above Schwinger critical field ($1.32 \times 10^{18}$ V/m). In addition to high field physics, TW X-ray pulses are required for single particle imaging [10].

Recently X-ray focusing capabilities to single nm scale have been extensively explored at SACLA using KB-mirrors [11,12]. We envision this technique will be extended to high power X-ray pulses in the near future, making the presented study feasible. Such experimental infrastructure, when built, would allow many new fundamental physics experiments, previously impossible, and therefore owing the main motivation for our research.

## DOUBLE-BUNCH FEL (DBFEL)

In our proposed experimental scheme, shown in Fig. 1, we consider two bunches generated at the photocathode, spaced 1.05 ns, or three RF-buckets, apart. The two bunch separation is determined by the real-estate constraints of the HXR electron beam chicane; see Fig. 1. The two bunches are accelerated and compressed using LCLS copper linac, to yield 15 fs flat-top bunch duration and 4 kA beam current. First bunch is expended after lasing in the first 7 undulators, while the second bunch, propagated initially off-axis, is overlapped with the radiation field in the tapered amplifier section. We will further refer to the system displayed in Fig. 1 as double-bunch FEL or DBFEL. For the detailed description of the DBFEL system, we refer the reader to [13]. The capability of producing and accelerating two bunches with LCLS copper linac has been repeatedly demonstrated in [14–16] for bunch separation in range of 0.35-200 ns. Measurements of the relative two bunch time jitter were done for different separations and found to be less than 10 fs. An analysis of a dataset for 50 ns bunch separation is presented in Fig. 2, where we found the timing jitter to be 5.9 fs RMS.

## NUMERICAL STUDIES OF DBFEL

The first step in studying the DBFEL is ELEGANT simulation of the LCLS Cu linac transport line, including linac wakefields and compression [17]. The resulting electron beam distribution is then converted and passed to the FEL code GENESIS [18] wrapped into additional package for analysis and tapering optimization [19]. A detailed numerical study, assuming given electron beam parameters, was done in our recent paper [13]. Here we only give a brief summary of the start-to-end simulation results.

After propagating through the SASE section (first 7 LCLS-II HXR undulators), the maximum SASE power for 4 keV photons is about 6 GW. It is then reduced to about 150 MW after the $C^*(111)$ monochromator and delayed and overlapped with the second bunch. Figure 3 illustrates the XFEL power as a function of distance in the LCLS-II HXR undulator for 4 keV photons.

With 1.05 ns separation, the second bunch is subject to longitudinal and transverse wakefields introduced by the first bunch. The effect of the longitudinal wakefield (monopole kick) can be compensated by tuning the phase of the laser at the photocathode [13, 14]. Transverse wakefield in the leading order can be calculated by using an expression from [20]: $W_y(t) = \sum 2\kappa_{y1n} \sin(2\pi f_{1n} t) e^{-\pi f_{1n} t/Q_{1n}}$, where $f_{1n}$ and $\kappa_{y1n}$ are the modes' frequencies and kick parameters respectively, and $Q_{1n} \approx 18000$. A plot of the long-range

ISBN: 978-3-95450-208-0 doi:10.18429/JACoW-IPAC2019-TUPRB088

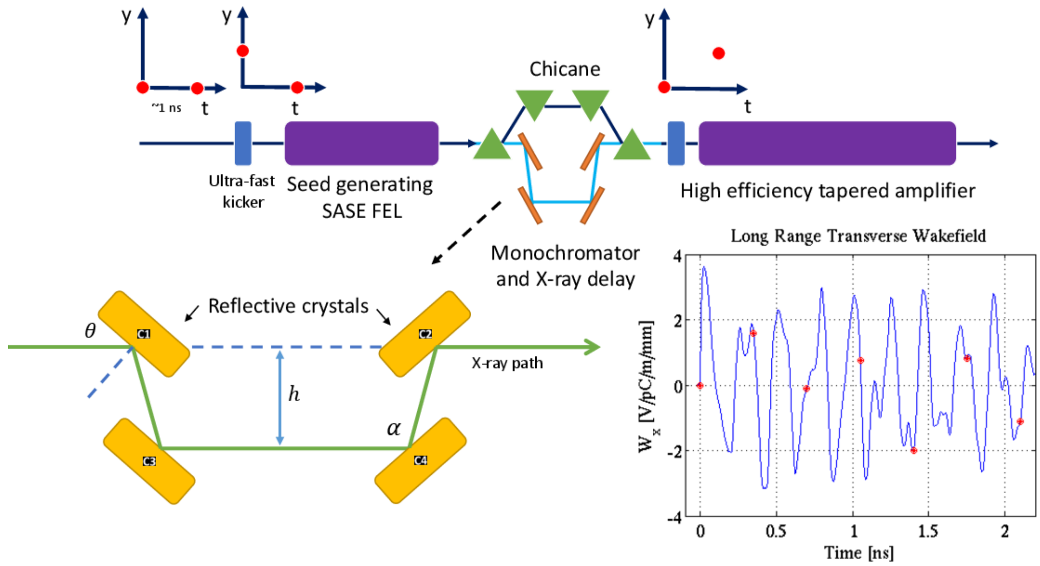


Figure 1: Double bunch X-ray FEL (DBFEL) setup (top) and four-crystal monochromator schematics (bottom left). Long range wakefield in LCLS copper linac as a function of bunch separation (bottom right).

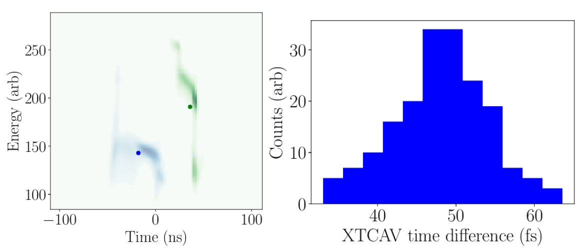


Figure 2: An example of double bunch XTCAV image (left) and a histogram of 200 images revealing an RMS relative time jitter of 5.9 fs (right).

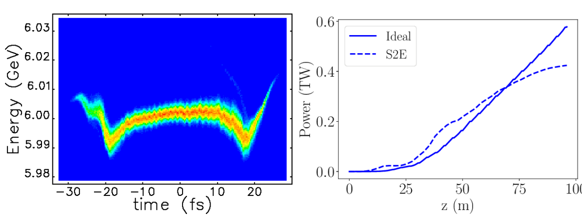


Figure 3: Longitudinal phase-space (LPS) of 4 kA 6 GeV beam (left). XFEL peak power in DBFEL scheme for 4 keV photons (right).

transverse wakefield kick is shown in Fig. 1. For a given LCLS copper linac length it translates into 1 µrad transverse slope of the second bunch induced by a maximum transverse displacement of the first bunch of 0.1 mm. Left uncorrected, with a betatron function of 20 m, it yields 20 µm maximum displacement, comparable to the RMS spotsize of the second bunch. However, since only one bunch needs to be on-axis per undulator section, the displacement can be corrected with dipole correctors, similar to split undulator schemes [21].

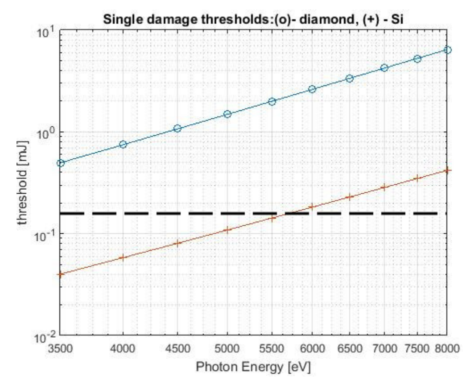


Figure 4: Instantaneous damage thresholds as a function of XFEL photon energy. Dashed line is expected SASE FEL performance.

## FOUR CRYSTAL MONOCHROMATOR

Currently, LCLS-II HXR self-seeding scheme utilizes forward Bragg diffraction as the seed X-rays. In this proceeding, we consider four-crystal Bragg reflection monochromator to perform double-bunch self-seeding [22]. A four-bounce system offers high seed power due to high reflectivity of the crystals, narrow bandwidth and tunability over large photon energy range. We chose type IIa single crystal diamonds with different lattice orientations to be accommodated in our setup. Diamond crystals are more resilient than Silicon to XFEL radiation damage, and provide better reflectivity in the photon range of 4-8 keV. For nominal operation of the four crystal monochromator, we consider the (1,1,1) lattice orientation.

The time delay in the monochromator is given by a simple relation $c\Delta\tau = 2h\tan\theta$, where $\theta$ is the Bragg angle, and $h$ is the lateral size; see Fig. 1. The longitudinal distance between two lower crystals is $\Delta_z = L - 2c\Delta\tau(\cot^2\theta/4 - 1/4)$.

ISBN: 978-3-95450-208-0 doi:10.18429/JACoW-IPAC2019-TUPRB088

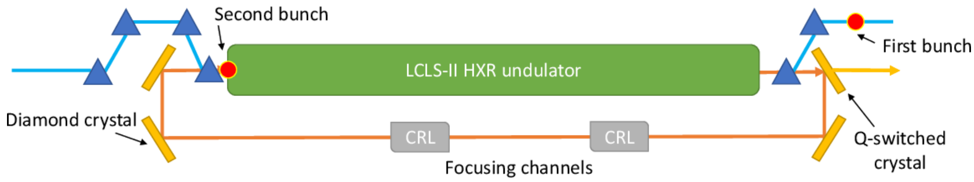


Figure 5: Cavity based DBFEL configuration, where the bunches are separated by 933 ns.

We note that in our setup the first crystal (C1) will be irradiated with the full SASE bandwidth and absorb/transit 97% of the XFEL power, estimated to be about 150 µJ per pulse. Crystals C2-C4 will only be subjected to narrow bandwidth radiation of 2-3% power level of the original pulse. In order to keep radiation trajectory parallel to the beam propagation direction, one has to ensure crystals C1-C2 are under identical thermal conditions and the effects of crystallographic lattice thermal expansion are mitigated. We calculated the instantaneous damage threshold that ensures the instantaneously delivered heat is below graphitization level of the diamond. For comparison, we provide the same calculation for Silicon in Fig. 4. The maximum delivered energy per pulse for 4 keV photons is about 0.1 mJ, thus well under instantaneous damage threshold for $C^*$. Our analysis suggests that due to excellent heat conductivity and low absorption, diamond crystals would operate under safe conditions at all designed photon energies for 120 Hz repetition rate.

## RECTANGULAR CAVITY-BASED MONOCHROMATOR

In order to take advantage of full HXR undulator length, we consider a scheme where crystal monochromator encompasses the entire undulator in a form of rectangular cavity, identical to regenerative amplifier FEL (RAFEL) scheme [24]; see Fig. 5. In this scheme, the X-ray photon energy is determined by the Bragg angle for crystals in the rectangular cavity to be equal to $\theta = 45°00'$.

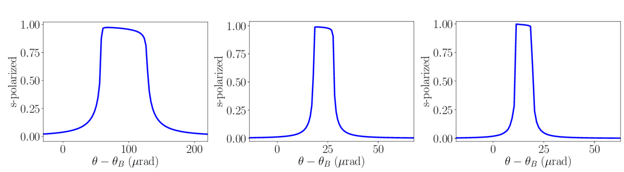


Figure 6: Rocking curves obtained from XOP code [23] for Diamond (1,1,1) at 4.2 keV (left), Diamond (3,1,1) at 8 keV (center) and Diamond (4,0,0) at 9.8 keV (right).

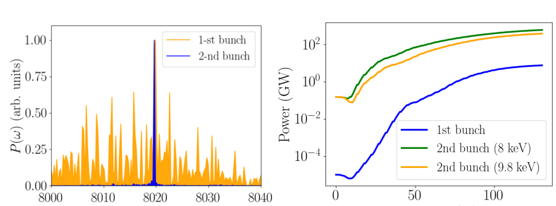


Figure 7: XFEL spectrum and peak power in DBFEL rectangular cavity monochromator for 8 keV and 9.8 keV photons.

Figure 6 shows rocking curves for 4.2 keV, 8 keV and 9.8 keV respectively. Note that tolerances in crystal alignment become significantly smaller due to Darwin width reduction at higher photon energies; see Fig. 6. While cavity-based DBFEL does not offer tunability, it can increase HXR power. We confirmed this with numerical simulations; see Fig. 7. In our simulations, the taper profile of HXR undulator was fixed and optimized for the second bunch. First bunch generated SASE in tapered undulator, and iteratively, taper profile was improved. Electron beam parameters correspond to the operational LCLS copper linac performance (0.4 µm emittance, 4 kA peak current, and 2.5 MeV energy spread). Figure 7 shows with a cavity-based monochromator wrapping entire undulator yields up to 700 GW of XFEL power in 8-9.8 keV photon energy range. This concept is a topic of active research.

## SUMMARY

In summary, we presented a scheme for generation of a very high peak power X-rays in the photon energy range of 4-8 keV by increasing the seeding power with a four-crystal $C^*(111)$ monochromator delay line. Stronger seeding also enhances the XFEL spectrum, as we pointed out in [13]. We also considered a DBFEL scheme where entire undulator is wrapped in a rectangular cavity, and confirmed it could enable near-TW HXR pulses. The success of cavity based monochromator is dependent on the implementation of the outcoupling mechanism with the diamond, which is actively investigated.

## ACKNOWLEDGEMENTS

This work was supported by the U.S. Department of Energy Contract No. DE-AC02-76SF00515. The authors are grateful to A. Marinelli, Y. Feng, H.-D. Nuhn, J. Wu, C. Mayes (SLAC), K.-J. Kim, Y. Shvydko (ANL) for useful discussions.

## REFERENCES

[1] G. A. Mourou, T. Tajima, and S. V. Bulanov, "Optics in the relativistic regime", *Rev. Mod. Phys.*, vol. 78, pp. 309–371, 2006.

[2] M. Marklund and P. K. Shukla, "Nonlinear collective effects in photon-photon and photon-plasma interactions", *Rev. Mod. Phys.*, 78:591–640, (2006).

[3] N. Kroll, P. Morton, and M. Rosenbluth, "Free-electron lasers with variable parameter wigglers", *IEEE Journal of Quantum Electronics*, vol. 17, iss. pp. 1436–1468, 1981.

ISBN: 978-3-95450-208-0 doi:10.18429/JACoW-IPAC2019-TUPRB088

[4] G. Geloni, V. Kocharyan, and E. Saldin, "Scheme for generation of highly monochromatic X-rays from a baseline XFEL undulator", 2010. arXiv,physics.acc-ph:1003.2548

[5] Y. Ding, Z. Huang, and R. D. Ruth, "Two-bunch self-seeding for narrow-bandwidth hard x-ray free-electron lasers", *Phys. Rev. ST Accel. Beams*, vol. 13, pp. 060703, 2010.

[6] G. Geloni, V. Kocharyan, and E. Saldin, "Extension of self-seeding scheme with single crystal monochromator to lower energy <5 keV as a way to generate multi-TW scale pulses at the European XFEL", 2012. arXiv,physics.acc-ph:1207.1981

[7] C. Emma, N. Sudar, P. Musumeci, A. Urbanowicz, and C. Pellegrini, "High efficiency tapered free-electron lasers with a prebunched electron beam", *Phys. Rev. Accel. Beams*, vol. 20, pp. 110701, 2017.

[8] C. Emma, Y. Feng, D. C. Nguyen, A Ratti, and C. Pellegrini, "Compact double bunch x-ray free electron lasers for fresh bunch self-see and harmonic lasing", *Phys. Rev. Acc. and Beams*, vol. 20, pp. 030701–10, 2017.

[9] C. Emma, K. Fang, J. Wu, and C. Pellegrini, "High efficiency, multiterawatt x-ray free electron lasers", *Phys. Rev. Accel. Beams*, vol. 19, pp. 020705, 2016.

[10] A. Aquila *et al.*, "The linac coherent light source single particle imaging road map", *Structural Dynamics*, vol. 2, iss. 4, pp. 041701, 2015.

[11] H. Mimura *et al.*, "Breaking the 10nm barrier in hard-X-ray focusing", *Nature Physics*, vol. 6, pp. 122–125, 2010.

[12] K. Yamauchi *et al.*, "Single-nanometer focusing of hard x-rays by kirkpatrick-baez mirrors", *Journal of Physics: Condensed Matter*, vol. 23, iss. 39, pp. 394206, 2011.

[13] A. Halavanau, F.-J. Decker, C. Emma, J. Sheppard, and C. Pellegrini, "Very high brightness and power LCLS-II hard X-ray pulses', *J. Synchrotron Rad.*, vol. 26, pp. 635–646, 2019. doi:10.1107/S1600577519002492

[14] F. J. Decker et al. In *Proceedings of FEL2010, Malmoe, Sweden*, page 467, (2010).

[15] F.-J. Decker, *et al* In *Proceedings, 37th International Free Electron Laser Conference (FEL 2015): Daejeon, Korea*, page WEP023, (2015).

[16] F.-J. Decker, K. L. F. Bane, W. S. Colocho, A. A. Lutman, and J. C. Sheppard, "Recent Developments and Plans for Two Bunch Operation with up to 1 µs Separation at LCLS", in *Proc. FEL'17*, Santa Fe, NM, USA, Aug. 2017, pp. 288–291. doi:10.18429/JACoW-FEL2017-TUP023

[17] M. Borland, "elegant: A Flexible SDDS-Compliant Code for Accelerator Simulation", APS, LS-287, 2000.

[18] S. Reiche. "GENESIS 1.3: a fully 3D time-dependent FEL simulation code", *Nuclear Instruments and Methods in Physics Research A*, vol. 429, pp. 243–248, 1999.

[19] C. Mayes and A. Halavanau. "lume-genesis package", *lume-genesis package*, https://github.com/slaclab/lume-genesis

[20] K Bane, "Wakefield calculations for the lcls in multibunch operation", SLAC-PUB-16039, 2011.

[21] C. Emma, A. Lutman, M. W. Guetg, J. Krzywinski, A. Marinelli, J. Wu, and C. Pellegrini, "Experimental demonstration of fresh bunch self-seeding in an x-ray free electron laser", *Applied Physics Letters*, vol. 110, no. 15, pp. 154101, 2017.

[22] Taito Osaka, *et al*, "A micro channel-cut crystal X-ray monochromator for a self-seeded hard X-ray free-electron laser", 2018. arXiv,physics.ins-det:1811.01860

[23] M. Sanchez del Rio and R. J. Dejus, "Status of XOP: v2.4: recent developments of the x-ray optics software toolkit", *SPIE Proceedings*, vol. 8141, pp. 814115, 2011. doi:10.1117/12.893911

[24] Z. Huang and R. D. Ruth, "Fully coherent X-ray pulses from a regenerative amplifier free electron laser", *Phys. Rev. Lett.*, vol. 96, pp. 144801, 2006.